



Published in final edited form as:

Oncogene. 2015 August 27; 34(35): 4664–4672. doi:10.1038/onc.2014.391.

Matriptase promotes inflammatory cell accumulation and progression of established epidermal tumors

Katiuchia Uzzun Sales^{1,2,3}, Stine Friis^{1,4}, Loreto Abusleme¹, Niki M. Moutsopoulos¹, and Thomas H. Bugge¹

¹Oral and Pharyngeal Cancer Branch, National Institute of Dental and Craniofacial Research, National Institutes of Health, Bethesda, MD, USA

²Clinical Research Core, National Institute of Dental and Craniofacial Research, National Institutes of Health, Bethesda, MD, USA

³Department of Cell and Molecular Biology, Ribeirao Preto School of Medicine, University of Sao Paulo, Ribeirao Preto, SP, Brazil

⁴Department of Cellular and Molecular Medicine, Faculty of Health and Medical Science, University of Copenhagen, Copenhagen, Denmark

Abstract

Deregulation of matriptase is a consistent feature of human epithelial cancers and correlates with poor disease outcome. We have previously shown that matriptase promotes multi-stage squamous cell carcinogenesis in transgenic mice through dual activation of pro-hepatocyte growth factor-cMet-Akt-mTor proliferation/survival signaling and PAR-2-Gαi-NFκB inflammatory signaling. Matriptase was congenitally and constitutively deregulated in our prior studies, and therefore it was unclear if aberrant matriptase signaling supports only initiation of tumor formation or if it is also critical for the progression of established tumors. To determine this, we here have generated triple-transgenic mice with constitutive deregulation of matriptase and simultaneous inducible expression of the cognate matriptase inhibitor, hepatocyte growth factor inhibitor (HAI)-2. As expected, constitutive expression of HAI-2 suppressed the formation of matriptase-dependent tumors in 7,12-Dimethylbenz(a)anthracene (DMBA)-treated mouse skin. Interestingly, however, the induction of HAI-2 expression in already established tumors markedly impaired malignant progression and caused regression of individual tumors. Tumor regression correlated with reduced accumulation of tumor-associated inflammatory cells, likely caused by diminished expression of pro-tumorigenic inflammatory cytokines. The data suggest that matriptase-dependent signaling may be a therapeutic target for both squamous cell carcinoma chemoprevention and for the treatment of established tumors.

Users may view, print, copy, and download text and data-mine the content in such documents, for the purposes of academic research, subject always to the full Conditions of use:http://www.nature.com/authors/editorial_policies/license.html#terms

Address correspondence to: Thomas H. Bugge, Ph.D., Oral and Pharyngeal Cancer Branch, National Institute of Dental and Craniofacial Research, National Institutes of Health, 30 Convent Drive, Room 211, Bethesda, MD 20892, Phone: (301) 435-1840, Fax: (301) 402-0823, thomas.bugge@nih.gov.

Conflict of Interest

Authors have declared that no competing interests exist.

Keywords

hepatocyte growth factor activator inhibitor-2; matriptase; oncogenic protease signaling; squamous cell carcinoma; tumor regression

Introduction

The membrane-anchored serine protease, matriptase, has gathered considerable attention in the context of human carcinogenesis, because it is deregulated with unusually high frequency in the epithelial compartment of human carcinomas of diverse origin, because its expression is negatively correlated with clinical outcome in several human carcinomas and certain hematopoietic malignancies, and because matriptase promotes tumorigenesis in several animal models (1–22). In regard to the latter, we have previously shown that low-level, constitutive expression of matriptase in the basal keratinocyte compartment of transgenic mice suffices to induce spontaneous *ras*-independent multistage squamous cell carcinogenesis and to potentiate *ras*-dependent malignant transformation induced by 7,12-Dimethylbenz(a)anthracene (DMBA) (22). Malignant transformation of squamous epithelium, including DMBA-induced transformation of mouse epidermis, is a sequential process that occurs through distinct stages that include hyperplasia, dysplasia, papilloma, carcinoma *in situ*, invasive carcinoma, and metastatic disease (23). The contribution of deregulated matriptase activity to early stage squamous cell carcinogenesis was established in our previous studies by the lack of any pre-malignant progression in bi-transgenic mice that constitutively overexpress matriptase along with the cognate matriptase inhibitor, hepatocyte growth factor activator inhibitor (HAI)-1 (22). However, whether the membrane-anchored serine protease also supports late-stage progression of squamous cell carcinogenesis has not been determined. In this study, we therefore generated triple-transgenic mice with constitutive deregulation of matriptase and simultaneous inducible expression of the potent cognate matriptase inhibitor, hepatocyte growth factor activator inhibitor (HAI)-2 (19, 24, 25), specifically in matriptase overexpressing cells. This inducible expression of HAI-2 enabled the acute blunting of matriptase activity after epidermal tumors were established. Using this novel experimental setup, we now show that matriptase is a critical promoter of late stages of squamous cell carcinoma progression and induces pro-tumorigenic chemokine and cytokine release, and inflammatory cell accumulation into established tumors. Taken together, these data indicate that matriptase may be a suitable therapeutic target for both squamous cell carcinoma chemoprevention and for the treatment of established tumors.

Results and Discussion

To determine the stage-specific contribution of matriptase in squamous cell carcinogenesis, we generated two novel transgenic mouse strains. The first strain constitutively expressed an HA epitope-tagged murine *Spint2* cDNA (encoding HAI-2) under control of the bovine keratin-5 promoter, hereafter referred to as *K5-Spint2*⁺⁰ mice (figure 1a and b, data are shown for one established transgenic line used for all further experiments). Reverse transcriptase (RT)-PCR analysis of mRNA from skin extracts showed that *K5-Spint2* mice

displayed an increase in total *Spint2* mRNA (figure 1b, compare lanes 1 with 2–4 and 5–7). This resulted in a marked increase in total epidermal HAI-2, as determined by Western blot using mouse HAI-2 antibodies (figure 1d, top panel, compare lanes 1 and 3). We next crossed *K5-Spint2*⁺⁰ mice to previously generated *K5-St14*⁺⁰ mice expressing a murine matriptase (*St14*) cDNA under control of the bovine keratin-5 promoter (22) to generate bi-transgenic *K5-St14*⁺⁰; *K5-Spint2*⁺⁰ mice and their single-transgenic and wildtype littermates (figure 1c). Western blot analysis showed that HAI-2 was well expressed in the bi-transgenic *K5-St14*⁺⁰; *K5-Spint2*⁺⁰ mice (figure 1d, top panel, compare lanes 3 and 4). Likewise, Western blot analysis using a matriptase antibody that recognizes the C-terminal serine protease domain showed that the level of total and activated epidermal matriptase was unaffected by the level of expression of HAI-2 (figure 1e, top panel, compare lanes 1 with 3 and 2 with 4). Finally, double immunofluorescence analysis using antibodies against the HA epitope tag of the transgenic HAI-2 fusion protein and antibodies against matriptase showed widespread co-localization of HAI-2 with matriptase in the basal keratinocyte compartment (compare figure 1f with i, g with j, examples with arrows in k).

To determine if constitutive HAI-2 expression impairs matriptase-dependent squamous cell carcinoma initiation, we next subjected the skin of cohorts of *K5-St14*⁺⁰; *K5-Spint2*⁺⁰ bi-transgenic mice and their associated *K5-St14*⁺⁰, *K5-Spint2*⁺⁰, and wildtype littermates to topical treatment with DMBA and followed tumor formation by outward inspection for 30 weeks (figure 1l). As previously reported (22, 26, 27), DMBA treatment did not result in tumor formation in wildtype mice (figure 1l, red lines). In sharp contrast, all mice overexpressing matriptase in basal keratinocytes developed tumors within seven weeks of treatment (figure 1l, blue lines) in agreement with previous studies (22). As described previously for HAI-1 (22), the rapid tumor formation caused by matriptase overexpression in basal keratinocytes was significantly blunted by the simultaneous overexpression of HAI-2 (figure 1l, green lines). No histological differences were apparent between tumors arising in *K5-St14*⁺⁰ single transgenic mice and *K5-St14*⁺⁰; *K5-Spint2*⁺⁰ bi-transgenic mice (figure 1m and n, data not shown). Importantly, transgenic HAI-2 remained well expressed in the DMBA-induced tumors and co-localized with tumor cell-expressed matriptase, as determined by immunofluorescence with antibodies against matriptase and the HA epitope (figure 1o–t, examples with arrows in t) showing that transgenic HAI-2 is co-localized with matriptase in DMBA-induced tumors when expressed under the control of a keratin-5 promoter.

To investigate the role of matriptase in the later stages of squamous cell carcinoma progression, we next generated a second transgenic mouse line in which matriptase is constitutively expressed under the control of the Keratin-5 promoter and in which HAI-2 was also expressed in a Keratin-5 promoter-dependent, but in an inducible manner. For this purpose, we first generated a transgenic mouse strain in which the HA-tagged *Spint2* cDNA was expressed under the control of a tetracycline-inducible promoter (Figure 2a, hereafter *pBig-Spint2*⁺⁰ mice). Studies in HEK293 cells confirmed that HAI-2 expression from this promoter was efficiently induced by the tetracycline-analogue, doxycycline, specifically in cells expressing a tetracycline transactivator (rtTA) protein consisting of the *E. coli* TetR (tetracycline repressor) fused to the Herpes Simplex Virus VP16 transactivation domain (28)

(figure 2b). Southern blot using genomic DNA from wildtype and transgenic mice showed a successfully inserted fragment compatible in size with the *Spint2* cDNA (figure 1c, lane 2). Consistent with this, when the *pBig-Spint2^{+/-0}* mice were crossed to previously generated *K5-TetOn^{+/-0}* mice expressing the rtTA protein under the control of the bovine keratin-5 promoter (29), HAI-2 expression could be specifically induced in the basal keratinocyte compartment by administration of doxycycline-containing chow to the ensuing *pBig-Spint2^{+/-0}; K5TetOn^{+/-0}* bi-transgenic mice (figure 2d, examples with arrowheads in right panel).

The *pBig-Spint2^{+/-0}; K5TetOn^{+/-0}* bi-transgenic mice next were crossed to *K5-St14^{+/-0}* mice to generate triple-transgenic *pBig-Spint2^{+/-0}; K5TetOn^{+/-0}; K5-St14^{+/-0}* mice. The mice were then subjected to DMBA treatment as described above to induce skin tumor formation (figure 3a). Once tumors emerged, the mice were randomly assigned to two groups. The first group continued to be fed normal chow, whereas the second group was fed doxycycline-containing chow to induce HAI-2 expression. Both treatment groups then were followed for an additional 14 weeks, and the change in tumor multiplicity and total tumor burden was then enumerated (figure 3b–e). As expected, a prolific progression of tumors was observed in mice fed normal chow. The median increase in tumor multiplicity was 6.5 and the median increase in total tumor burden was 0.4 g (figure 3d and e, golden squares). As also expected, all tumors visible at study initiation increased in size (examples with arrows in figure 3b and b'). Interestingly, however, tumor progression in mice fed doxycycline-containing chow was markedly blunted, with an increase in median tumor multiplicity of just 1 and an increase in median total tumor burden of just 0.05 g (figure 3d and e, red squares). Furthermore, tumors visible at study initiation often displayed obvious regression, indicative of a specific requirement of matriptase activity for continued tumor growth (examples with arrowheads in figure 3c and c'). Immunofluorescence analysis of tumors from doxycycline-fed and control mice using antibodies against the HA epitope tag of the HAI-2 fusion protein and antibodies against matriptase showed induction of HAI-2 expression by doxycycline and frequent colocalization of HAI-2 with matriptase in tumor cells (figure 1f–k, compare f with i and g with j). HAI-2 expression, however, was generally patchy, with some areas of the tumors showing intense staining (figure 3i, arrowheads) and other areas being devoid of staining. This non-homogeneous induction of HAI-2 provides a likely explanation for the relatively unimpeded growth of some tumor nodules and the occasional emergence of new tumors during doxycycline administration.

To mechanistically dissect how matriptase promotes the progression of established tumors, we performed a comparative histological analysis of tumor lesions and adjacent hyperplastic tissue of mice fed normal or doxycycline-containing chow (figure 4a–p). No significant effect of HAI-2 induction was observed on tumor cell proliferation (figure 4m). Interestingly, however, macrophage (examples in a–d, quantification in figure 4n), neutrophil (examples in figure 4e–h, quantification in figure 4o), and T lymphocyte infiltration (examples in figure 4i–l, quantification in 4p) into the tumors, as determined by, respectively, Mac1 [Cd11b], myeloperoxidase (MPO), and CD3 antibodies, were all significantly diminished, suggesting that HAI-2 induction impairs matriptase-dependent pro-inflammatory signaling. To investigate this, we analyzed the levels of the key keratinocyte

pro-inflammatory chemokine and cytokine genes, *chemokine (C-X-C motif) ligand 1* (*Cxcl1*), *thymic stromal lymphopoietin* (*Tslp*), and *colony stimulating factor 2 (granulocyte-macrophage)* (*Csf2*) in newborn *K5-St14^{+/-0}*; *K5-Spint2^{+/-0}* bi-transgenic mice and their *K5-St14^{+/-0}*, *K5-Spint2^{+/-0}*, and wildtype littermates (figure 4q-s). We chose to analyze the three chemokine/cytokine genes because they were previously shown to be induced by matriptase in skin tumors (26), and we chose newborn mice because the skin is histologically normal at birth (22) and differences in cytokine expression, therefore, are more likely to be a direct consequence of matriptase-mediated inflammatory signaling. All three cytokine or chemokine genes displayed markedly increased expression in *K5-St14^{+/-0}* mice as compared to wildtype littermates, although significance only was obtained for *Cxcl1* (figure 4q-s, blue squares, compare with brown squares). Interestingly, however, this matriptase-mediated increase in inflammatory cytokine expression was abrogated by simultaneous HAI-2 expression (figure 4q-s, compare purple squares to brown and blue squares). Taken together, these data suggest that matriptase promotes the progression of established epidermal tumors at least in part through induction of pro-tumorigenic inflammatory cytokines.

Trypsin-like serine proteases with their extracellular location and well-known mechanism of catalysis and zymogen activation are long-established as excellent drug targets (30). The capacity of genetic downregulation of matriptase activity to induce stasis or regression of established tumors that we demonstrated in this study uncovers a critical contribution of the protease also to late stages of squamous cell carcinoma progression, and illustrates the potential utility of its pharmacological targeting for both squamous cell carcinoma chemoprevention and treatment of established tumors. Thus, even epidermal tumors in which *ras* is activated by topical DMBA application (22, 31-34) remained dependent on matriptase proteolytic activity for further expansion and often regressed in its absence. The exact cellular mechanism by which this tumor regression occurred remains to be established. We did not observe obvious differences in tumor cell proliferation, apoptosis (data not shown) or necrosis (data not shown), although it is conceivable that the histological procedures used to assess these parameters may not be sufficiently sensitive to detect subtle changes. Alternatively, tumor regression may be a rapid process that is not captured in the collected tumor samples. We previously identified two matriptase-dependent signaling pathways that each is essential for initiating malignant transformation of squamous epithelium: a) A cMet-Akt-mTor proliferation/survival signaling pathway, initiated by matriptase cleavage of keratinocyte cell surface-bound pro-hepatocyte growth factor, and, b) a Gai-NFκB inflammatory signaling pathway, initiated by matriptase cleavage of keratinocyte protease-activated receptor-2 (26, 27). The marked reduction in the abundance of tumor-associated inflammatory cells observed after matriptase inhibition in established tumors would suggest that protease-activated receptor-2-dependent pro-inflammatory signaling represents at least one molecular component of matriptase-promotion of late stage carcinogenesis. However, matriptase also has been proposed to promote progression of other cancers through the activation of pro-macrophage-stimulating protein 1/pro-hepatocyte-like growth factor (35), receptor bound pro-urokinase plasminogen activator (36-38), src-associated transmembrane protein SIMA135/CDCP1/TRASK (39), and platelet-derived growth factor-D (40).

A considerable number of small molecule and macromolecular inhibitors of matriptase have been developed (41–48). The data presented in this paper should further stimulate ongoing efforts towards the development and use of inhibitors of matriptase for human cancer treatment.

Acknowledgments

We thank Dr. Mary Jo Danton and Dr. J. Silvio Gutkind for critically reviewing this manuscript. We also thank Andrew Cho and Dr. Ashok Kulkarni, NIDCR Gene Targeting Facility, for generation of transgenic mice. Histology was performed by Histoserv, Inc., Germantown, MD. The study was supported by the NIDCR Intramural Research Program (THB), Sao Paulo Research Foundation 2014/14311-0 (KUS), The Harboe Foundation, The Foundation of 17.12.1981, and the Lundbeck Foundation (SF)

References

1. Cheng MF, Huang MS, Lin CS, Lin LH, Lee HS, Jiang JC, et al. Expression of matriptase correlates with tumour progression and clinical prognosis in oral squamous cell carcinoma. *Histopathology*. 2014; 65(1):24–34. [PubMed: 24382204]
2. Ha SY, Kim KY, Lee NK, Kim MG, Kim SH. Overexpression of matriptase correlates with poor prognosis in esophageal squamous cell carcinoma. *Virchows Archiv : an international journal of pathology*. 2014; 464(1):19–27. [PubMed: 24248283]
3. Baba T, Kawaguchi M, Fukushima T, Sato Y, Orikawa H, Yorita K, et al. Loss of membrane-bound serine protease inhibitor HAI-1 induces oral squamous cell carcinoma cells' invasiveness. *The Journal of pathology*. 2012; 228(2):181–92. [PubMed: 22262311]
4. Bergum C, List K. Loss of the matriptase inhibitor HAI-2 during prostate cancer progression. *The Prostate*. 2010; 70(13):1422–8. [PubMed: 20687215]
5. Bocheva G, Rattenholl A, Kempkes C, Goerge T, Lin CY, D'Andrea MR, et al. Role of matriptase and proteinase-activated receptor-2 in nonmelanoma skin cancer. *J Invest Dermatol*. 2009; 129(7):1816–23. [PubMed: 19242518]
6. Nakamura K, Abarzua F, Hongo A, Kodama J, Nasu Y, Kumon H, et al. Hepatocyte growth factor activator inhibitor-2 (HAI-2) is a favorable prognosis marker and inhibits cell growth through the apoptotic pathway in cervical cancer. *Annals of oncology : official journal of the European Society for Medical Oncology/ESMO*. 2009; 20(1):63–70. [PubMed: 18689863]
7. Jin JS, Cheng TF, Tsai WC, Sheu LF, Chiang H, Yu CP. Expression of the serine protease, matriptase, in breast ductal carcinoma of Chinese women: correlation with clinicopathological parameters. *Histol Histopathol*. 2007; 22(3):305–9. [PubMed: 17163404]
8. Vogel LK, Saebo M, Skjelbred CF, Abell K, Pedersen ED, Vogel U, et al. The ratio of Matriptase/HAI-1 mRNA is higher in colorectal cancer adenomas and carcinomas than corresponding tissue from control individuals. *BMC Cancer*. 2006; 6:176. [PubMed: 16820046]
9. Saleem M, Adhami VM, Zhong W, Longley BJ, Lin CY, Dickson RB, et al. A novel biomarker for staging human prostate adenocarcinoma: overexpression of matriptase with concomitant loss of its inhibitor, hepatocyte growth factor activator inhibitor-1. *Cancer Epidemiol Biomarkers Prev*. 2006; 15(2):217–27. [PubMed: 16492908]
10. Jin JS, Hsieh DS, Loh SH, Chen A, Yao CW, Yen CY. Increasing expression of serine protease matriptase in ovarian tumors: tissue microarray analysis of immunostaining score with clinicopathological parameters. *Mod Pathol*. 2006; 19(3):447–52. [PubMed: 16439987]
11. Zeng L, Cao J, Zhang X. Expression of serine protease SNC19/matriptase and its inhibitor hepatocyte growth factor activator inhibitor type 1 in normal and malignant tissues of gastrointestinal tract. *World J Gastroenterol*. 2005; 11(39):6202–7. [PubMed: 16273651]
12. Tanimoto H, Shigemasa K, Tian X, Gu L, Beard JB, Sawasaki T, et al. Transmembrane serine protease TADG-15 (ST14/Matriptase/MT-SP1): expression and prognostic value in ovarian cancer. *Br J Cancer*. 2005; 92(2):278–83. [PubMed: 15611789]

13. Hoang CD, D’Cunha J, Kratzke MG, Casmey CE, Frizelle SP, Maddaus MA, et al. Gene expression profiling identifies matriptase overexpression in malignant mesothelioma. *Chest*. 2004; 125(5):1843–52. [PubMed: 15136399]
14. Santin AD, Cane S, Bellone S, Bignotti E, Palmieri M, De Las Casas LE, et al. The novel serine protease tumor-associated differentially expressed gene-15 (matriptase/MT-SP1) is highly overexpressed in cervical carcinoma. *Cancer*. 2003; 98(9):1898–904. [PubMed: 14584072]
15. Kang JY, Dolled-Filhart M, Ocal IT, Singh B, Lin C-Y, Dickson RB, et al. Tissue microarray analysis of HGF/met pathway components reveals a role for Met, matriptase, and HAI-1 in the progression of node-negative breast cancer. *Cancer Research*. in press.
16. Oberst MD, Johnson MD, Dickson RB, Lin CY, Singh B, Stewart M, et al. Expression of the serine protease matriptase and its inhibitor HAI-1 in epithelial ovarian cancer: correlation with clinical outcome and tumor clinicopathological parameters. *Clin Cancer Res*. 2002; 8(4):1101–7. [PubMed: 11948120]
17. Chou FP, Chen YW, Zhao XF, Xu-Monette ZY, Young KH, Gartenhaus RB, et al. Imbalanced matriptase pericellular proteolysis contributes to the pathogenesis of malignant B-cell lymphomas. *The American journal of pathology*. 2013; 183(4):1306–17. [PubMed: 24070417]
18. Ye, j; kawaguchi, M.; Haruyama, y; Kanemaru, a; Fukushima, y; Yamamoto, K., et al. Loss of hepatocyte growth factor activator inhibitor type 1 participates in metastatic spreading of human pancreatic cancer cells in a mouse orthotopic transplantation model. *Cancer Science*. 2014; 105(1): 44–51. [PubMed: 24147538]
19. Tsai CH, Teng CH, Tu YT, Cheng TS, Wu SR, Ko CJ, et al. HAI-2 suppresses the invasive growth and metastasis of prostate cancer through regulation of matriptase. *Oncogene*. 2013
20. Wu SR, Cheng TS, Chen WC, Shyu HY, Ko CJ, Huang HP, et al. Matriptase is involved in ErbB-2-induced prostate cancer cell invasion. *The American journal of pathology*. 2010; 177(6): 3145–58. [PubMed: 20971737]
21. Cheng H, Fukushima T, Takahashi N, Tanaka H, Kataoka H. Hepatocyte growth factor activator inhibitor type 1 regulates epithelial to mesenchymal transition through membrane-bound serine proteinases. *Cancer Res*. 2009; 69(5):1828–35. [PubMed: 19223533]
22. List K, Szabo R, Molinolo A, Sriuranpong V, Redeye V, Murdock T, et al. Deregulated matriptase causes ras-independent multistage carcinogenesis and promotes ras-mediated malignant transformation. *Genes Dev*. 2005; 19(16):1934–50. [PubMed: 16103220]
23. Yuspa SH. The pathogenesis of squamous cell cancer: lessons learned from studies of skin carcinogenesis. *J Dermatol Sci*. 1998; 17(1):1–7. [PubMed: 9651822]
24. Szabo R, Hobson JP, Christoph K, Kosa P, List K, Bugge TH. Regulation of cell surface protease matriptase by HAI2 is essential for placental development, neural tube closure and embryonic survival in mice. *Development*. 2009; 136(15):2653–63. [PubMed: 19592578]
25. Szabo R, Hobson JP, List K, Molinolo A, Lin CY, Bugge TH. Potent inhibition and global co-localization implicate the transmembrane Kunitz-type serine protease inhibitor hepatocyte growth factor activator inhibitor-2 in the regulation of epithelial matriptase activity. *The Journal of biological chemistry*. 2008; 283(43):29495–504. [PubMed: 18713750]
26. Sales, KU.; Friis, S.; Konkel, JE.; Godiksen, S.; Hansen, KK.; Szabo, R., et al. Non-hematopoietic PAR-2 is essential for matriptase-driven pre-malignant progression and potentiation of ras-mediated squamous cell carcinogenesis. 2013. Submitted
27. Szabo R, Rasmussen AL, Moyer AB, Kosa P, Schafer J, Molinolo A, et al. c-Met-induced epithelial carcinogenesis is initiated by the serine protease matriptase. *Oncogene*. 2011; 30:2003–16. [PubMed: 21217780]
28. Gossen M, Bujard H. Tight control of gene expression in mammalian cells by tetracycline-responsive promoters. *Proc Natl Acad Sci U S A*. 1992; 89(12):5547–51. [PubMed: 1319065]
29. Vitale-Cross L, Amornphimoltham P, Fisher G, Molinolo AA, Gutkind JS. Conditional expression of K-ras in an epithelial compartment that includes the stem cells is sufficient to promote squamous cell carcinogenesis. *Cancer Res*. 2004; 64(24):8804–7. [PubMed: 15604235]
30. Lopez-Otin C, Bond JS. Proteases: multifunctional enzymes in life and disease. *The Journal of biological chemistry*. 2008; 283(45):30433–7. [PubMed: 18650443]

31. Balmain A, Pragnell IB. Mouse skin carcinomas induced in vivo by chemical carcinogens have a transforming Harvey-ras oncogene. *Nature*. 1983; 303(5912):72–4. [PubMed: 6843661]
32. Balmain A. Transforming ras oncogenes and multistage carcinogenesis. *Br J Cancer*. 1985; 51(1): 1–7. [PubMed: 3881118]
33. Quintanilla M, Brown K, Ramsden M, Balmain A. Carcinogen-specific mutation and amplification of Ha-ras during mouse skin carcinogenesis. *Nature*. 1986; 322(6074):78–80. [PubMed: 3014349]
34. Ise K, Nakamura K, Nakao K, Shimizu S, Harada H, Ichise T, et al. Targeted deletion of the H-ras gene decreases tumor formation in mouse skin carcinogenesis. *Oncogene*. 2000; 19(26):2951–6. [PubMed: 10871846]
35. Bhatt AS, Welm A, Farady CJ, Vasquez M, Wilson K, Craik CS. Coordinate expression and functional profiling identify an extracellular proteolytic signaling pathway. *Proc Natl Acad Sci U S A*. 2007
36. Takeuchi T, Harris JL, Huang W, Yan KW, Coughlin SR, Craik CS. Cellular localization of membrane-type serine protease 1 and identification of protease-activated receptor-2 and single-chain urokinase-type plasminogen activator as substrates. *The Journal of biological chemistry*. 2000; 275(34):26333–42. [PubMed: 10831593]
37. Lee SL, Dickson RB, Lin CY. Activation of hepatocyte growth factor and urokinase/plasminogen activator by matriptase, an epithelial membrane serine protease. *The Journal of biological chemistry*. 2000; 275(47):36720–5. [PubMed: 10962009]
38. Kilpatrick LM, Harris RL, Owen KA, Bass R, Ghorayeb C, Bar-Or A, et al. Initiation of plasminogen activation on the surface of monocytes expressing the type II transmembrane serine protease matriptase. *Blood*. 2006; 108(8):2616–23. [PubMed: 16794252]
39. Bhatt AS, Erdjument-Bromage H, Tempst P, Craik CS, Moasser MM. Adhesion signaling by a novel mitotic substrate of src kinases. *Oncogene*. 2005; 24(34):5333–43. [PubMed: 16007225]
40. Ustach CV, Huang W, Conley-LaComb MK, Lin CY, Che M, Abrams J, et al. A novel signaling axis of matriptase/PDGF-D/ss-PDGFR in human prostate cancer. *Cancer Res*. 2010; 70(23):9631–40. [PubMed: 21098708]
41. Enyedy IJ, Lee SL, Kuo AH, Dickson RB, Lin CY, Wang S. Structure-based approach for the discovery of bis-benzamidines as novel inhibitors of matriptase. *J Med Chem*. 2001; 44(9):1349–55. [PubMed: 11311057]
42. Long Y, Lee S, Lin C, Enyedy IJ, Wang S, Li P, et al. Synthesis and evaluation of the sunflower derived trypsin inhibitor as a potent inhibitor of the type II transmembrane serine protease, matriptase. *Bioorg Med Chem Lett*. 2001; 11(18):2515–9. [PubMed: 11549459]
43. Sun J, Pons J, Craik CS. Potent and selective inhibition of membrane-type serine protease 1 by human single-chain antibodies. *Biochemistry*. 2003; 42(4):892–900. [PubMed: 12549907]
44. Galkin AV, Mullen L, Fox WD, Brown J, Duncan D, Moreno O, et al. CVS-3983, a selective matriptase inhibitor, suppresses the growth of androgen independent prostate tumor xenografts. *The Prostate*. 2004; 61(3):228. [PubMed: 15368474]
45. Forbs D, Thiel S, Stella MC, Sturzebecher A, Schweinitz A, Steinmetzer T, et al. In vitro inhibition of matriptase prevents invasive growth of cell lines of prostate and colon carcinoma. *Int J Oncol*. 2005; 27(4):1061–70. [PubMed: 16142324]
46. Desilets A, Longpre J-M, Beaulieu M-E, Leduc R. Inhibition of human matriptase by eglin c variants. *FEBS Lett*. 2006; 580(9):2227–32. [PubMed: 16566926]
47. Quimbar P, Malik U, Sommerhoff CP, Kaas Q, Chan LY, Huang Y-H, et al. High-affinity cyclic peptide matriptase inhibitors. *The Journal of biological chemistry*. 2013; 288(19):13885–96. [PubMed: 23548907]
48. Gray K, Elghadban S, Thongyoo P, Owen KA, Szabo R, Bugge TH, et al. Potent and specific inhibition of the biological activity of the type-II transmembrane serine protease matriptase by the cyclic microprotein MCoTI-II. *Thromb Haemost*. 2014; 112(2):402–11. [PubMed: 24696092]
49. Murillas R, Larcher F, Conti CJ, Santos M, Ullrich A, Jorcano JL. Expression of a dominant negative mutant of epidermal growth factor receptor in the epidermis of transgenic mice elicits striking alterations in hair follicle development and skin structure. *Embo J*. 1995; 14(21):5216–23. [PubMed: 7489711]

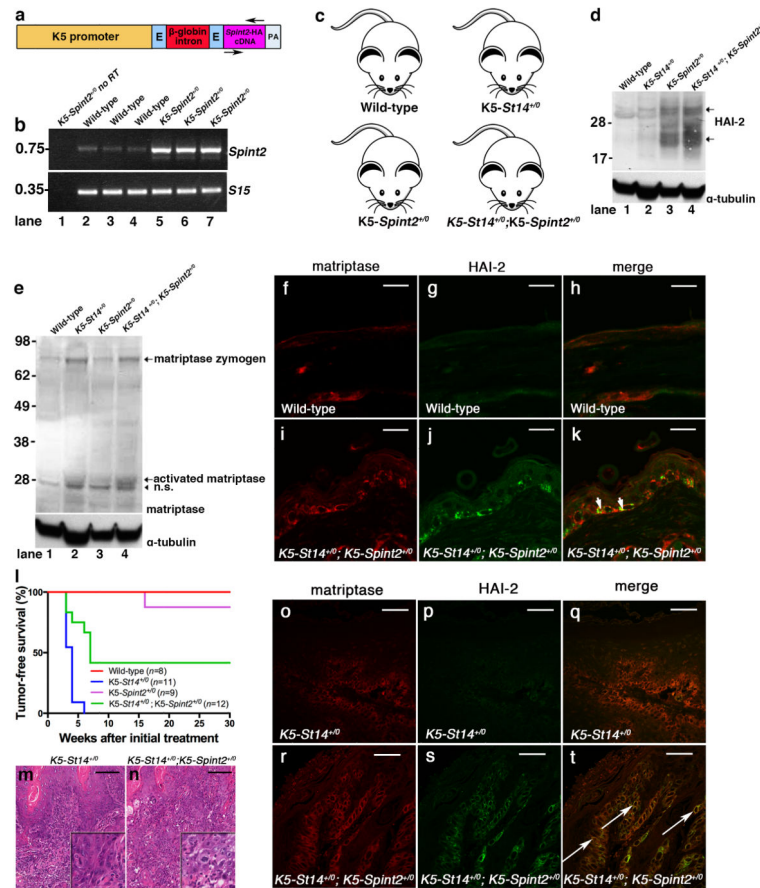


Figure 1. Constitutive HAI-2 expression in basal keratinocytes inhibits matriptase-dependent squamous cell carcinogenesis initiation

(a–k) Generation of constitutive keratin-5-*Spint2* transgenic mice. (a) Schematic structure of the *K5-Spint2* transgene with the insertion of the full-length murine *Spint2* cDNA (NP_001076017.1) containing a synthetic DNA sequence encoding a C-terminal human influenza hemagglutinin (HA)-Tag (YPYDVPDYA) just prior to the stop codon inserted into a unique *NotI* site of the vector pBK5 (49). Bovine keratin-5 promoter (K5 promoter, yellow), rabbit β -globin exons (E, light blue), rabbit β -globin intron (red), mouse *Spint2*-HA cDNA (purple) and rabbit β -globin polyadenylation signal (PA, grey). Positions of primers used for mouse genotyping and RT-PCR analysis are indicated (arrows). The linearized transgene vector was microinjected into the male pronucleus of FVB/NJ zygotes, which then were implanted into pseudopregnant mice. *Spint2* transgenic founders were identified by Southern blot hybridization of *NotI*-digested genomic DNA using a 32 P-labeled 600 bp probe spanning the entire *Spint2* cDNA. The *Spint2* transgenic lines were maintained in the hemizygous state (*K5-Spint2*^{+/-}) in an FVB/NJ background and were genotyped by PCR using genomic DNA from tail biopsies with the following primer pairs: 5'-ATATATGCGGCCGCGCCACCATGGCGCAGCTTTGTGAGCTG-3' and 5'-ATATATGCGGCCGCTTAGGCATAGTCAGGCACGTCATAAGGATACAAGAC-3'. (b) Expression of *Spint2* mRNA in epidermis of wildtype mice (lanes 2–4) and *K5-Spint2*^{+/-} (lanes 5–7) littermates using RT-PCR analysis for *Spint2* and ribosomal protein S15. No RT

was added to lane 1. *Spint2* mRNA is increased in the epidermis of *K5-Spint2^{+/-}* transgenic mice. Whole skin was snap-frozen in liquid nitrogen and ground to a fine powder with mortar and pestle. Total RNA was prepared by extraction in Trizol reagent (Life Technologies, Grand Island, NY) as recommended by the manufacturer. Reverse transcription and PCR amplification were performed using the High-Capacity cDNA Reverse Transcription Kit (Life Technologies), as recommended by the manufacturer. **(c)** Mice were interbred in order to generate bi-transgenic *K5-St14^{+/-}*; *K5-Spint2^{+/-}* mice and the associated single-transgenic and wildtype littermate controls. **(d)** Expression of HAI-2 in epidermis of wildtype (lane 1), *K5-St14^{+/-}* (lane 2), *K5-Spint2^{+/-}* (lane 3) and *K5-St14^{+/-}*; *K5-Spint2^{+/-}* (lane 4) mice as determined by Western blot using HAI-2 antibodies (AF1107, R&D Systems). HAI-2 has a predicted molecular weight of 28 kDa, however, a larger 32 kDa and a smaller 20 kDa band (arrows) is also present likely due to variable post-translational processing of the protein. Western blot of α -tubulin is shown in the bottom panel as loading control. **(e)** Expression of matriptase zymogen (70 kDa) and activated matriptase (30 kDa) in epidermis of wildtype (lane 1), *K5-St14^{+/-}* (lane 2), *K5-Spint2^{+/-}* (lane 3), and *K5-St14^{+/-}*; *K5-Spint2^{+/-}* (lane 4) mice, as determined by reducing Western blot using anti-matriptase antibodies. Positions of matriptase zymogen and activated matriptase are shown. N.S. indicates non-specific band. Western blot of α -tubulin is shown in the bottom panel as loading control. Epidermal protein extracts were prepared by homogenizing the tissue in ice-cold lysis buffer (1% Triton X-100, 0.5% Sodium-deoxycholate in phosphate buffered saline (PBS) plus Proteinase Inhibitor Cocktail (Sigma, St. Louis, MO) and incubated on ice for 10 min. The lysates were spun and the supernatant was mixed with 4 \times SDS sample buffer (NuPAGE, Invitrogen) containing 7% β -mercaptoethanol and boiled for 10 min. The proteins were separated on a 4–12% BisTris NuPage gel and transferred to a 0.2- μ m pore size PVDF membrane (Invitrogen). The membrane was blocked with 5% nonfat dry milk in tris-buffered saline (TBS) containing 0.05% Tween 20 (TBS-T) for 1 h at room temperature. The membrane was probed with anti-matriptase antibody (AF3946, R&D Systems) diluted in 1% nonfat dry milk in TBS-T overnight at 4 °C. The next day, the membrane was washed three times for 5 min each in TBS-T and incubated for 1 h with alkaline phosphatase-conjugated secondary antibodies (Thermo Scientific, Waltham, MA). After three 5-min washes with TBS-T, the signal was developed using nitro blue tetrazolium/5-bromo-4-chloro-3-indolyl phosphate solution (Pierce). **(f–k)** Co-expression of transgenic HAI-2 and matriptase in basal keratinocytes of *K5-St14^{+/-}*; *K5-Spint2^{+/-}* bi-transgenic mice. Wildtype (f–h) and *K5-St14^{+/-}*; *K5-Spint2^{+/-}* (i–k) skin samples were analyzed by immunofluorescence using antibodies against matriptase (f and i) and HA-tag for HAI-2 (g and j). Matriptase and HAI-2 expression co-localize in cells of the basal layer of the epidermis (merge, h and k, arrows in k). Skin samples from mice were fixed in 4% paraformaldehyde in PBS for 24 h, embedded into paraffin, and sectioned. Tissue sections were cleared with xylene-substitute, rehydrated in a graded series of alcohols, and boiled in Reduced pH Retrieval Buffer (Bethyl, Montgomery, TX) for 20 min for antigen retrieval. The sections were blocked for 1 h in PBS containing 10% horse serum and incubated at 4°C overnight with sheep-anti matriptase (AF3946, R&D Systems) and rabbit-anti-HA (H6908, Sigma) for detection of transgenic HAI-2. The slides were washed 3 times for 5 min with 3% BSA in PBS and 0.1% Triton X-100 and incubated at room temperature for 1 h with Alexa fluor 594-labeled donkey anti-sheep and FITC-

labeled goat-anti-rabbit antibodies (Zymed). Tissue sections then were washed 3 times for 5 min with PBS and mounted with VectaShield Hard set Mounting Medium (Vector Laboratories Inc., Burlingame, CA). The samples were subjected to laser scanning confocal microscopy using the Leica TCS SP2 system and Zeiss LS700 system. **(l)** Kaplan-Meier analysis of tumor-free survival of littermate *K5-St14^{+/-0}*; *K5-Spint2^{+/-0}* (n=12, green), *K5-St14^{+/-0}* (n=11, blue), *K5-Spint2^{+/-0}* (n=9, purple), and wildtype (n=8, red) mice. The mice received 5 treatments of 250 µg/ml DMBA in acetone every 3 weeks. The mice were monitored for up to 30 weeks for tumor formation. $P < 0.0001$, *K5-St14^{+/-0}* versus other genotypes (log-rank test, two-tailed). The experiments were performed in an Association for Assessment and Accreditation of Laboratory Animal Care International-accredited vivarium following Institutional Guidelines and standard operating procedures. **(m and n)** Representative hematoxylin and eosin stained sections of squamous cell carcinoma at low and high (insets) magnification in *K5-St14^{+/-0}* (m) and *K5-St14^{+/-0}*; *K5-Spint2^{+/-0}* (n) transgenic mice 6 weeks after initiation of DMBA treatment. The histological appearance of tumors is similar irrespective of genotype. Size bars = 100 µm. Skin and tumor tissues were fixed for 24 h in 4% paraformaldehyde in phosphate buffered saline, processed into paraffin, sectioned into sagittal 3-µm sections and stained with hematoxylin and eosin prior to histopathological assessment. **(o-t)** *K5-St14^{+/-0}* (o-q) and *K5-St14^{+/-0}*; *K5-Spint2^{+/-0}* (r-t) squamous cell carcinoma samples were analyzed by immunofluorescence using antibodies against matriptase (o and r) and the HA-tag for HAI-2 (p and s). Matriptase and HAI-2 expression co-localize in tumor cells throughout the malignant tumor (merge, q and t, examples with arrows in q). Size bars = 50 µm. Immunofluorescence was performed as described above.

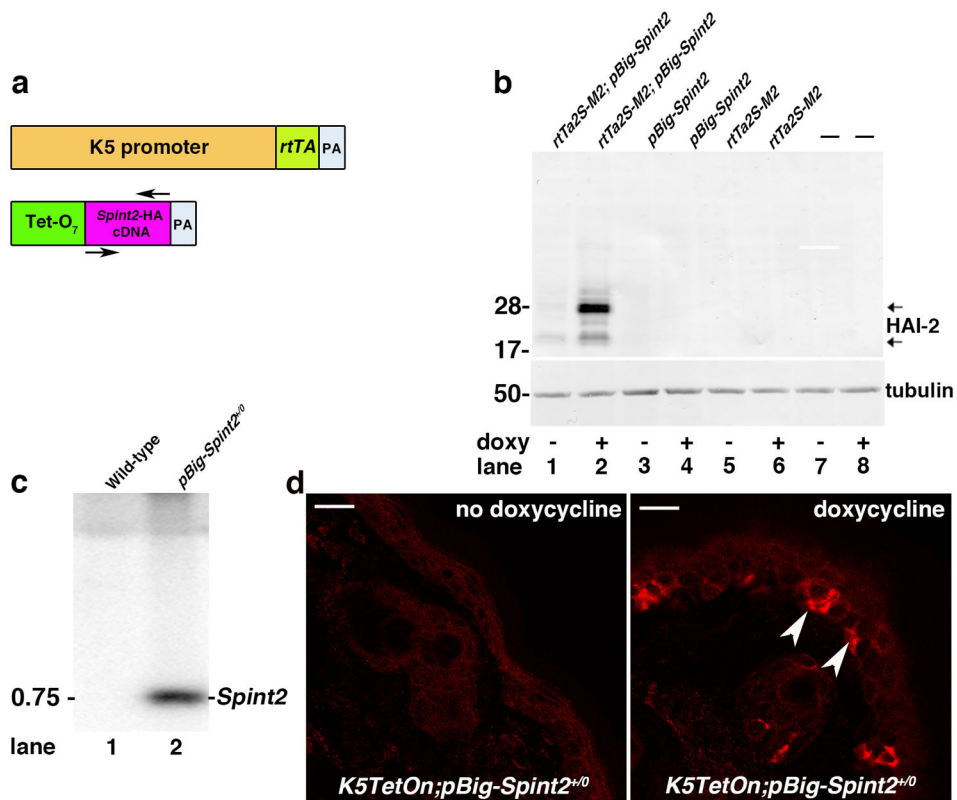


Figure 2. Generation of inducible *Spint2* transgenic mice

(a) Doxycycline-inducible *K5-Spint2* mice (*pBig-Spint2*^{+/0}). Tet-O₇-*Spint2*-HA transgene consisting of full-length murine *Spint2* cDNA, with a synthetic DNA sequence encoding a C-terminal HA-Tag, as described in figure 1, was inserted just prior to the stop codon into a unique NotI site of the pBig transgene expression vector placing the *Spint2* cDNA (purple) is under the control of seven *tet* responsive elements (Tet-O₇, green). Establishment and maintenance of transgenic mouse lines was performed as described in figure 1. (b) Western blot analysis of HAI-2 expression in HEK293 cells transfected either with doxycycline-inducible *rtTa2S-M2* tet-transactivator and *pBig-Spint2-HA* (lanes 1 and 2), with *pBig-Spint2-HA* alone (lanes 3 and 4), with *rtTa2S-M2* alone (lanes 5 and 6) or left untransfected (lanes 7 and 8), and then treated with doxycycline for 48 hr (lanes 2, 4, 6, and 8) or left untreated (lanes 1, 3, 5 and 7). HAI-2 is efficiently induced only in cells containing *rtTa2S-M2* (constitutively expressing the tetracycline transactivator) and *pBig-Spint2-HA* plasmids. HEK293 cells were grown in Dulbecco's modified Eagles medium (DMEM) supplemented with 2 mM L-glutamine, 10% fetal bovine serum, 100 units/ml penicillin, and 100 μg/ml streptomycin (Gibco, Life Technologies, Grand Island, NY) at 37 °C in an atmosphere of 5% CO₂. HEK293 cells were transfected using Turbofect (Thermo Scientific) according to the manufacturer's instructions, and then were treated with doxycycline for 48 hr or left untreated. Western blot analysis was performed as described in figure 1. (c) Southern-blot analysis of *NotI*-digested genomic DNA from wildtype (lane 1) and *pBig-Spint2*^{+/0} (lane 2) mice using a ³²P-labeled 600 bp probe spanning the entire *Spint2* cDNA confirmed the presence of the transgene in *pBig-Spint2*^{+/0} transgenic mice (marked as "*Spint2*" on the

right). Position of molecular weight marker (kb) is indicated on the left. **(d)** Inducible expression of HAI-2 in basal keratinocytes. Skin biopsies from a 5-week-old bi-transgenic mouse expressing a HA-tagged *Spint2* cDNA under control of a doxycycline-inducible promoter, and a *rtTA* transgene under control of a K5 promoter (*K5-TetOn^{+/0}; pBig-Spint2^{+/0}* mice) before (left panel) and after being fed doxycycline-containing chow (right panel) for 15 days. Note the patchy expression of transgenic HAI-2 (examples with arrowheads in right panel) in basal keratinocytes only after doxycycline-administration. Size bars = 20 μ m. Epidermal sections were analyzed by immunofluorescence using HA antibodies, as described in figure 1.

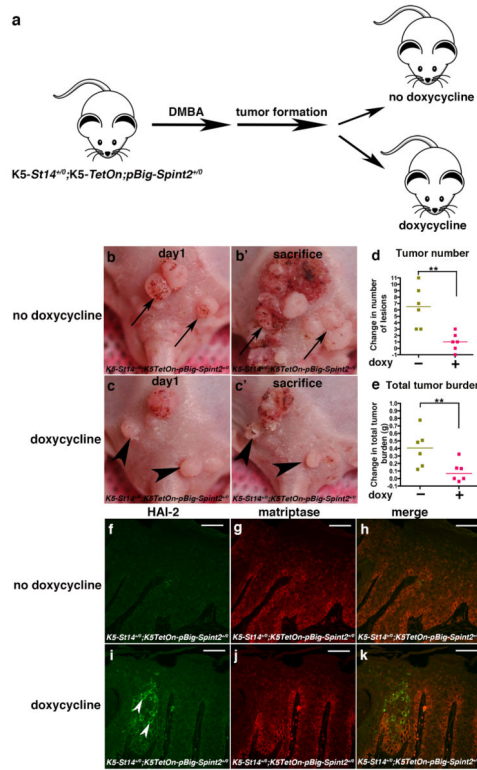


Figure 3. Matriptase promotes malignant progression subsequent to initial tumor formation (a) *K5-St14^{+0/0}*; *K5TetOn^{+0/0}* and *pBig-HAI-2^{+0/0}* mice were interbred in order to generate triple transgenic mice. Dorsal skin of *K5-St14^{+0/0}*; *K5TetOn^{+0/0}*; *pBig-HAI-2^{+0/0}* triple-transgenic mice were topically treated with 250 $\mu\text{g}/\text{ml}$ DMBA every three weeks. Once tumors were outwardly visible, the mice were randomized into two groups that were fed either doxycycline-containing chow (n=6) to induce HAI-2 expression in K5-expressing cells or were fed control chow (n=6) and observed for an additional 14 weeks (b–c') Representative examples of individual DMBA-treated *K5-St14^{+0/0}*; *K5TetOn^{+0/0}*; *pBig-HAI-2^{+0/0}* triple-transgenic mice before (b and c) and 3 weeks after (b' and c') being fed either normal chow (b and b') or fed doxycycline-containing chow (c and c'). Examples of progressing tumors in mouse fed normal chow is shown with arrows in b and b'. Examples of regressing tumors in mouse fed doxycycline-containing chow are shown with arrowheads in c and c'. (d and e) Change in number of tumors (d) and total tumor burden (e) in mice fed normal chow (golden squares) and in mice fed doxycycline-containing chow (red squares). Horizontal bars indicate median values ** $P < 0.002$ in d and $P < 0.005$ in e, Student's t-test, two-tailed. Doxycycline was administered with standard mouse chow at a concentration of 6 g/kg (Quality Lab Products, Baltimore, MD). (f–k) Immunofluorescent detection of transgenic HAI-2 using HA antibodies (f and i), matriptase immunofluorescence (g and j), and merged images (h and k) of tumors from DMBA-treated *K5-St14^{+0/0}*; *K5TetOn^{+0/0}*; *pBig-HAI-2^{+0/0}* triple-transgenic mice after being fed either normal chow (f–h) or doxycycline-containing chow (i–k) for 3 weeks. Examples of cells expressing transgenic HAI-2 are shown with arrowheads in i. Size bars = 50 μm . Immunofluorescence was performed as described in the legend to figure 1.

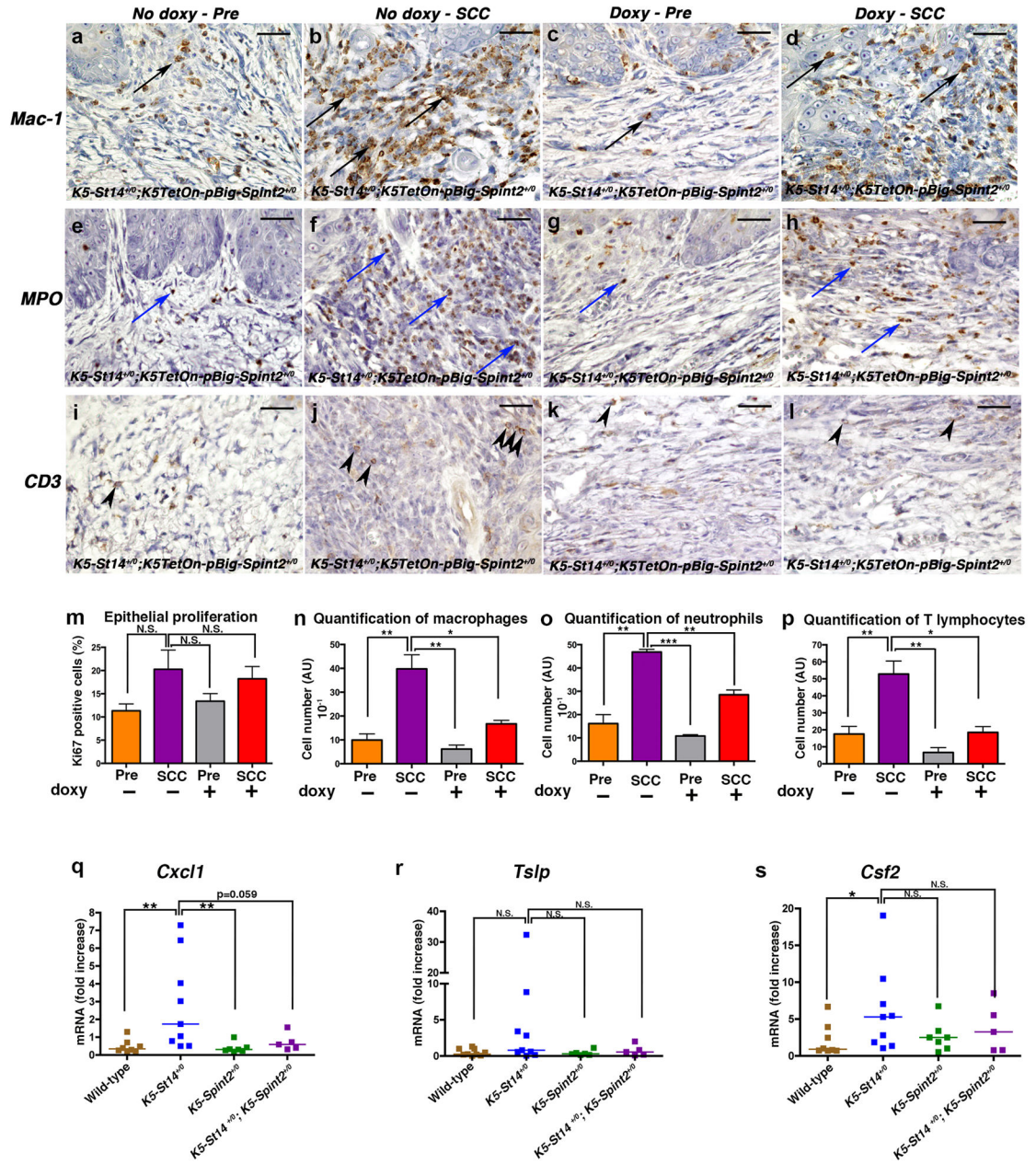


Figure 4. Inhibition of matriptase decreases inflammatory cell infiltration into established epidermal tumors

(a–p) Immunohistochemical analysis of DMBA-treated *K5-St14^{+/0}; K5TetOn^{+/0}; pBig-HAI-2^{+/0}* triple-transgenic mice treated with 5 doses of 250 µg/ml DMBA and fed either control chow or fed doxycycline-containing chow for 14 weeks to induce HAI-2 expression in K5-expressing cells. (a–l) Representative immunohistochemistry sections of hyperplastic epithelia and SCC lesions showing macrophages (Mac1, a–d, black arrows), neutrophils (MPO, e–h, blue arrows) and T lymphocytes (CD3, i–l, arrowheads). Increased recruitment of inflammatory cells is present in SCC lesions from mice fed normal chow as compared to mice fed doxycycline-containing chow. Bar sizes: 100 µm. (m–p) Immunohistochemical

analysis of DMBA-treated *K5-St14^{+/-0}*; *K5TetOn^{+/-0}*; *pBig-HAI-2^{+/-0}* triple-transgenic mice fed either control chow (n=3, orange and purple bars) or fed doxycycline-containing chow for 14 weeks (n=3, grey and red bars). Samples from hyperplastic skin adjacent to SCC lesions (Pre, orange and grey bars), and Squamous Cell Carcinoma (SCC, purple and red bars) were analyzed. (m) Enumeration of Ki-67-positive cells was used as a marker for cell proliferation. No statistical difference in tumor cell proliferation was observed amongst groups. P=N.S., SCC fed control chow *versus* all the other groups (Student's t-test, two-tailed). (n-p) Quantification of inflammatory cell infiltrates in hyperplastic skin and SCC, as described above, by enumeration of macrophages (n, Mac1 [Cd11b] antibodies), neutrophils (o, MPO antibodies) and T lymphocytes (p, CD3 antibodies). Densities of macrophages, neutrophils and T lymphocytes were significantly increased in tumors from mice that were fed normal chow when compared to mice fed doxycycline-containing chow to induce HAI-2 expression. *P<0.0198 and **P<0.0097 in n, **P<0.0016 and ***P<0.0001 in o, *P<0.0163 and **P<0.0048 in p, SCC fed control chow *versus* other groups (unpaired Student's t-test, two-tailed). Skin and tumor tissues were fixed for 24 h in 4% paraformaldehyde in phosphate buffered saline, processed into paraffin, cut into sagittal 3- μ m sections. Immunohistochemistry was performed using the following primary antibodies, anti-Ki-67 (Dako, Carpinteria, CA), anti-Mac1 [Cd11b] (Abcam, Cambridge, MA), anti-Myeloperoxidase (Abcam) and anti-CD3 (Abcam). After incubation with secondary antibodies, slides were developed using the diaminobenzidine substrate (Sigma-Aldrich), mounted and scanned using Scan Scope. (q-s) RNA was isolated from epidermis of 1-day-old wild type (brown squares, n=7), *K5-St14^{+/-0}* (blue squares, n=9), *K5-Spint2^{+/-0}* (green squares, n=7) and *K5-St14^{+/-0}*; *K5-Spint2^{+/-0}* (purple squares, n=5) mice. Quantification of *Cxcl-1* (q), *Tslp* (r), and *Csf2* (s) mRNA levels were performed by real-time PCR using TaqMan probes. *Cxcl-1*, *Tslp* and *Csf2* mRNA were all increased in the *K5-St14^{+/-0}* mice when compared to *K5-St14^{+/-0}*; *K5-Spint2^{+/-0}*; *K5-Spint2^{+/-0}* and wildtype littermates. **P<0.0025 in Q, P=N.S. in R, *P=0.0274 and P=N.S. in S, *K5-St14^{+/-0}* versus the other genotypes (Mann-Whitney U test, two-tailed). Reverse transcription was performed using the High-Capacity cDNA Reverse Transcription Kit (Life Technologies), as recommended by the manufacturer. *Cxcl1*, *Tslp* and *Csf2*q PCRs were done using TaqMan probes following the manufacturer's instructions (Life Technologies).